EFDA–JET–CP(10)01/07

L. Figini, P. Platania, D. Farina, S.Garavaglia, G Grossetti, S. Nowak, C. Sozzi
and JET EFDA contributors

Multi-Angle Measurement of EC Emission by Fast Electrons: Sensitivity Study

Multi-Angle Measurement of EC Emission by Fast Electrons: Sensitivity Study

L. Figini, P. Platania, D. Farina, S.Garavaglia, G Grossetti, S. Nowak, C. Sozzi
and JET EFDA contributors*

JET-EFDA, Culham Science Centre, OX14 3DB, Abingdon, UK

[1]IFP-CNR, EURATOM-ENEA-CNR Association, Milan, Italy
** See annex of F. Romanelli et al, "Overview of JET Results",*
(Proc. 22 [nd] IAEA Fusion Energy Conference, Geneva, Switzerland (2008)).

Preprint of Paper to be submitted for publication in Proceedings of the
16th Joint Workshop on Electron Cyclotron Emission and Electron Cyclotron Resonance Heating,
Sanya, China.
(12th April 2010 - 15th April 2010)

ABSTRACT.
Multiple angle (0, 10, 20 degrees with respect to the radial direction) and polarization (X, O modes) ECE spectra of JET plasmas with significant Lower Hybrid additional power were obtained with the Oblique ECE diagnostics. Such data have been analyzed with the emission code SPECE that encompasses a multi-Maxwellian model of the fast electron tail driven by Lower Hybrid waves. The model has been used to fit, varying the control parameters, the five experimental signals of the ECE diagnostic aiming to characterize the LH power absorption and driven current.

1. MOTIVATION AND ANALYSIS TOOLS

Electron Cyclotron Emission (ECE) is strongly dependent on the electron distribution function, and even a tiny fraction of the electron population having sufficient energy can introduce a significant deformation in the thermal ECE spectrum when the cold resonance lies outside the plasma volume. Downshifted second harmonic extraordinary (X) mode emission is a distinctive feature of ECE spectra in presence of energetic electrons, and the details of this feature are mainly related to the spatial location, the parallel momentum and the perpendicular temperature of the energetic electrons. The analysis of the suprathermal emission can thus reveal details of the mechanism sustaining the involved non-thermal electron fraction.

The Oblique ECE diagnostics of JET provides five simultaneous spectra (nominally 0° X mode, 10° and 20° X and O modes, where the angle refers to the radial direction) over an extended frequency range (70-350GHz), with spectral resolution up to 7GHz and time resolution of 5ms [1]. These spectra probe the electron distribution function at different electron energies thanks to the energy dependence of the resonance condition at different emission angles [2]. The data analyzed in this paper have been relatively calibrated following a careful procedure based on both absolutely calibrated data and on benchmarked simulations [3].

A simple multi-Maxwellian model [4] is included in the emission code SPECE [5] to describe the typical Lower Hybrid (LH) driven plateau in the electron distribution function (e.d.f.):

$$f(\psi,\vec{u}) = \left(1-\eta(\psi)\right)\cdot f_{M,T_b}\left(|\vec{u}|\right) + \eta(\psi)\sum_{i=1}^{N} f_{M,T_b}\left(|\vec{u}-\vec{u}_{//0,i}|\right) \tag{1}$$

where u=p/mc is the normalized momentum, ψ is the normalized poloidal flux coordinate, and T_b and T_{tail} are the temperatures of the Maxwellian distributions f_M in the bulk and in the tail respectively. The value of T_{tail} determines both the spread of the tail in $u_{||}$ and also the spacing in $u_{//}$ among the Maxwellians:

$$u_{//0,1} = \sqrt{T_b/mc^2}, \quad \Delta u_{//} = u_{//0,i} \quad u_{//0,i-1} = 2\sqrt{T_{tail}/mc^2} \tag{2}$$

The number of Maxwellians N can be chosen to control the extent of the suprathermal tail along the $u_{//}$ axis. A plateau extending up to the expected value $u_{//,max} \sim (N_{//,min}^2-1)^{-1/2}$, where $N_{//,min}$ is the minimum value of the parallel refraction index component in the launched wave spectrum, can be

approximated by choosing N such that

$$N = 1 + \mathrm{int}\left[\sqrt{mc^2/T_{tail}}\left(u_{//,\max} - u_{//0,1}\right)/2\right] \tag{3}$$

Finally, the density fraction of superthermal electrons η is assumed to be peaked at flux coordinate ψ_0 with peak value η_0 and gaussian decrease with width ψ_c:

$$\eta(\psi) = \eta_0 \cdot \exp\left[-(\psi - \psi_0)^2/\psi_c^2\right] \tag{4}$$

When the cold resonance for harmonic n = 2 is inside the plasma volume the plasma itself is optically thick due to interaction of the radiation with the bulk of low energy electrons, and the radiation temperature T_r corresponds to the bulk electron temperature T_b. The downshifted emission instead is visible when the cold resonance n = 2 is outside plasma volume: the number of interacting electrons is low and plasma is optically thin, so that the radiation temperature is $T_r \sim n_{tail}T_{tail}^2$. The spectral shape of the downshifted emission is dependent on the distribution in space and energy of the fast electrons, i.e., in the adopted model, it depends on $u_{//,max}$, T_{tail}, ψ_0, and ψ_c.

2. EXPERIMENTAL DATA

In order to characterize the dependence and sensitivity of the simulated spectra from the five parameters η_0, ψ_0, ψ_c, $u_{//,max}$, T_{tail} a database of JET pulses having a rather wide range of macroscopic parameters has been considered (see Table 1), in both transient and steady phases.

Figure 1 shows the experimental spectra for Pulse No: 77874 during the switching-on of the additional power (at the time of the analysis: $n_e = 7$, $P_{NBI} = 7$, $P_{LH} = 2$, $I_p = 1.8$, $B_0 = 2.66$, $N_{//} = 1.8$ in the units of Table 1). The experimental data are compared with the SPECE simulations obtained with the tail parameters reported in the caption, and the downshifted emission peak due to the tail of fast electron is visible around 110GHz.

3. SCAN OF THE TAIL'S PARAMETERS

Figure 2 shows the variation of suprathermal peak shape for the perpendicular emission while scanning the tail parameters, compared with the experimental data of JET Pulse No's: 74087 at t = 20.1s. When varying the spatial localization of the suprathermal population, the LH driven current has been kept unchanged at I_{LH}/I_p = 430kA/2MA. In Fig.2a and 2b the location and the width in space of the suprathermal population are varied respectively. Larger ψ_0 means fast electrons localization at more external radii, therefore the suprathermal emission has a lower peak (lower density) at lower frequency. Fig. 2c clearly shows that, for a given current I_{LH} localized around a given flux surface ψ_0, the ECE spectrum is almost insensitive to the width of the current channel (ψ_c). In Fig. 2c the tail temperature T_{tail} has been varied, keeping $\eta_0 T_{tail}$ = constant. The downshift effect increases with the T_{tail} value, which also affects the value of $u_{//,max}$ through equations (2) and (3). Therefore low T_{tail} also means low $u_{//,max}$. The N parameter (kept constant at N = 2 in the previous

cases) is varied in Fig.2d. In this case the scan is step-like, and the plateau extends approximately up to an energy

$$E_{\max} = mc^2(\gamma_{\max} - 1) = mc^2\left(\sqrt{1 + u_{//,\max}^2} - 1\right) \tag{5}$$

that, for $T_{tail} = 23$keV and N = 1, 2, 3 ($|u_{//,max}| = 0.2, 0.6, 1.0$), is about $E_{max} = 10$, 85, and 210keV respectively. This latter scan performed for the oblique views is shown in Figure 3. Both in perpendicular and oblique spectra, a large variation in the spectrum shape is associated to the lower N steps (low $u_{//,max}$ values), because at large N values the e.d.f. is modified in a region of the $u_{//}$, $u_{\wedge}$ space not involved in the resonance process. The energy range corresponding to the three lines of sight is shown in Figure 4: in the case shown, the oblique views are sensitive to lower electron energies with respect to the perpendicular view, and as a consequence the oblique spectra are less affected by changes in the energetic part of the tail.

4. MINIMAL DETECTABLE SUPRATHERMAL FRACTION

When the cold EC resonance lies in the optically thin plasma layer at the edge and a strong temperature gradient exists towards the hotter inner plasma, downshifted emission might be visible even in a purely Maxwellian plasma. This radiation is emitted by the energetic part of the Maxwellian population, and it might hide or add to the feature generated by a tail of fast electrons. In order to evaluate the minimal fraction of non-Maxwellian electrons that the diagnostic can detect, a case at high temperature where marginal LH wave coupling is expected (JET Pulse No: 77874) was analyzed. Assuming a Maxwellian edf, the simulated spectrum shown good agreement with the experimental data, well reproducing the downshifted feature too, as seen in Figure 5. We then introduced a fictitious suprathermal fraction, large enough to be visible beyond the experimental error bars. For a temperature $T_{tail} \sim 40$keV, the corresponding density of suprathermal electrons, carrying a current $I_{LH} \sim 50$kA, was found to be $n_{st} \sim 4\ 10^{15}\ m^{-3}$ ($\eta_0 \sim 0.01\%$).

CONCLUSIONS

Experimental data taken with ObECE diagnostics of JET have been analyzed using the emission code SPECE, in which a model for the LHCD driven emission is included. The parameter space of the model has been explored, showing that it is possible to derive information about the LHCD power localization and its current drive efficiency from the comparison between data and simulations.

ACKNOWLEDGMENTS

This work, carried out under the European Fusion Development Agreement, supported by the European Communities and “Istituto di Fisica del Plasma P.Caldirola – CNR”, has been carried out within the Contract of Association between EURATOM and IFP. The views and opinions expressed herein do not necessarily reflect those of the European Commission or IFP.

REFERENCES

[1]. C.Sozzi et al., AIP Conference Proceedings, vol. 988, (2008) 73

[2]. E. de la Luna et al., Review of Scientific Instruments 74, (2003) 1414 and V. Krivenski, Fusion Engineering Design 53, (2001) 23

[3]. L. Figini et al, submitted to Review Scientific Instruments

[4]. Brusati et al., Nuclear Fusion 34, (1994) 23

[5]. D.Farina et al. Conference Proceedings, vol. 988, (2008) 128

Pulse parameter	Min	Max
Vacuum field B_0 (T)	2.3	3.4
Plasma total current I_p (MA)	1.75	2.5
Integrated density n_e ($10^{19}/m^2$)	4.3	11
Electron bulk temperature $T_{e,b}$ (keV)	3	8
Superthermal rad. Temp. $T_{rad,st}$ (keV)	1	8
Additional power P_{add} (MW)	2	25
Lower Hybrid power P_{LH} (MW)	1.9	5
$N_{//}$ at LH's antenna	1.8	2.3

Table 1. Range of main parameters for the analyzed shots

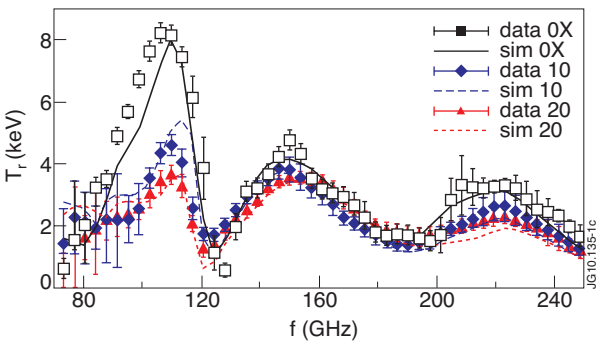

Figure 1: Experimental (open symbols) and simulated (lines) emission spectra at 0° (X mode), 10°, and 20° (O+X mode), for Pulse No: 77874 at t = 4.11s. Spectra are simulated with the following e.d.f. parameters: T_{tail} = 45keV, $u_{//,max} = -0.8$, $h_0 = 1.4\ 10^{-3}$, $\psi_0 = 0.3$, $\psi_c = 0.12$ (I_{LH} = 380kA). Error bars include calibration uncertainty and signal variance over 30ms time average.

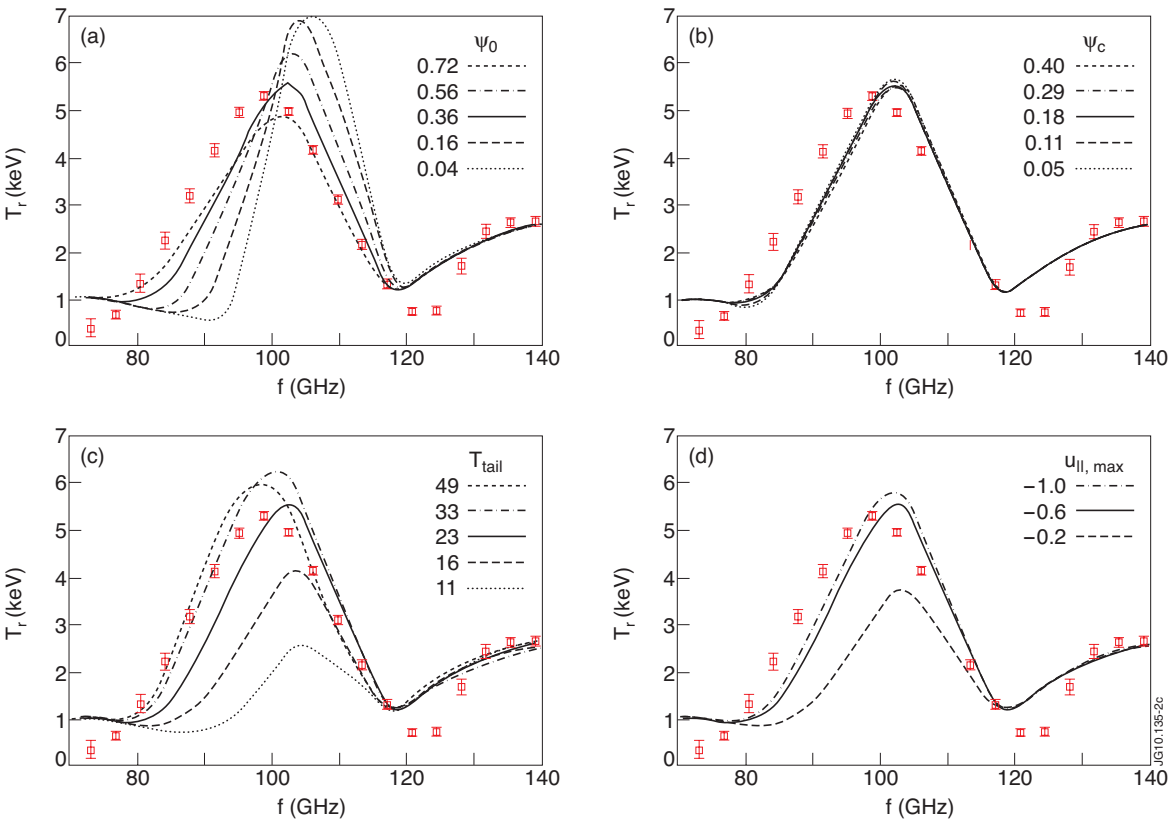

Figure 2: e.d.f. parameters scan around the estimated values for Pulse No: 74087 at t = 20.1s (T_{tail} = 23keV, $u_{//,max}$ = −0.6, $h_0 = 8.5\ 10^{-4}$, $\psi_0 = 0.56$, $\psi_c = 0.18$, I_{LH} = 430kA). Open symbols represent measured data at 0°, lines are simulated spectra. (a) ψ_0 scan, (b) ψ_c scan, (c) T_{tail} scan, (d) $u_{//,max}$ scan. When scanning a parameter, the other values are kept unchanged except: (a) ψ_c adjusted to keep the current channel width constant, η_0 rescaled to keep I_{LH} constant; (b) η_0 rescaled to keep I_{LH} constant; (c) h_0 rescaled to keep $\eta_0 T_{tail}$ constant; (d) h_0 rescaled to keep η_0/N constant.

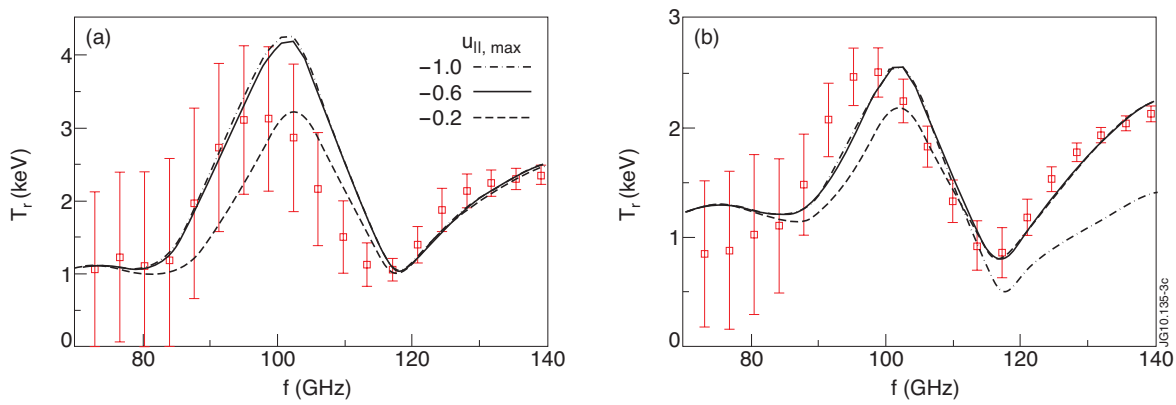

Figure 3: Same as Figure 2d for (a) 10° O+X spectrum, (b) 20° O+X spectrum.

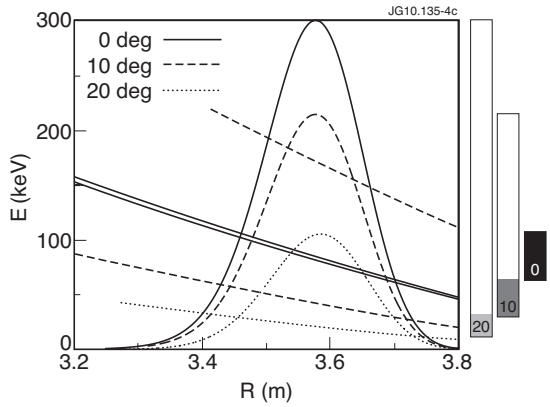

Figure 4: Emission profile $aT_{rad}exp(-t)$ (thin bell-shaped curves) for X mode at 0°, 10°, 20[, f = 102GHz, and respective resonance energy ranges (thick lines). Lower energies (E < 50keV) can be "seen" by oblique lines of sight only. Pulse No: 74087 at t = 20.1s, same parameters as Figure 2.

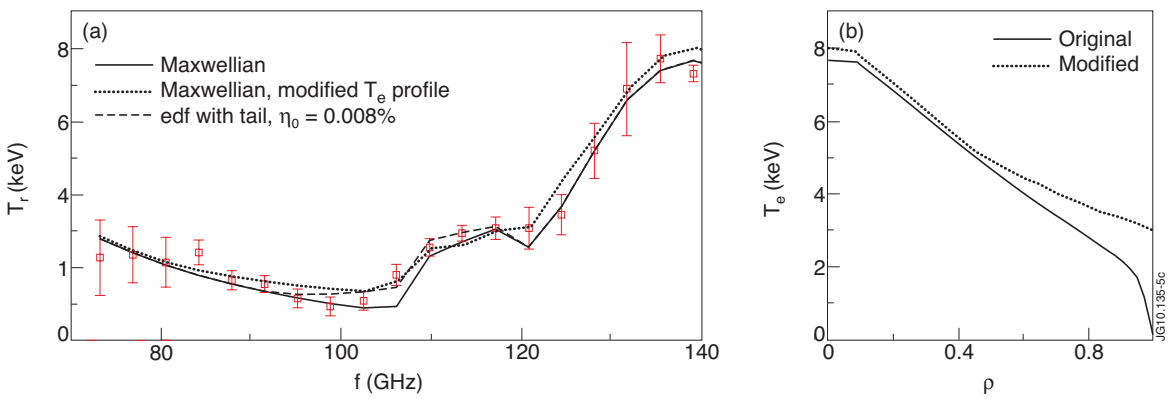

Figure 5: Downshifted emission feature in the perpendicular X mode spectrum (a) for Pulse No: 77874 at t = 6.0s. Measured data (symbols) are compared with spectra simulated either using Maxwellian e.d.f. and different T_e profiles (solid, dotted, profiles shown in (b)), or assuming an e.d.f. with a tail of fast electrons (dashed). e.d.f. parameters are indicated in Figure 1, except η_0 that has been scaled down ($\eta_0 = 8\ 10^{-5}$) to match the Maxwellian simulation within the error bars.